

DANISH CENTER FOR APPLIED
MATHEMATICS AND MECHANICS

by

Abstract:

Near-elastic vibro-impact analysis by discontinuous transformations and averaging

Jon Juel Thomsen^{a,*} and Alexander Fidlin^b

^a *Department of Mechanical Engineering, Solid Mechanics, Technical University of Denmark, Building 404, DK-2800 Lyngby, Denmark*

^b *LuK GmbH & Co. oHG, Industriestr. 3, D-77815, Buehl/Baden, Germany*

Abstract

We show that near-elastic vibro-impact problems can be conveniently analyzed by a discontinuity-reducing transformation of variables, combined with an extended averaging procedure that allows small discontinuities. A general technique for this is presented, and illustrated by calculating transient or stationary motions for different harmonic oscillators with stops or clearances, and self-excited friction oscillators with stops or clearances. First- and second-order analytical predictions are derived, and shown to agree to estimated accuracy with results of numerical simulation.

Keywords: nonlinear oscillations; vibro-impact; averaging; discontinuous transformation

1. Introduction

Vibro-impact systems are characterized by repeated impacts. Applications include devices to crush, grind, forge, drill, punch, tamp, pile, and cut a variety of objects, and vibrating machinery or structures with stops or clearances [1]. Also, vibro-impact is involved in noise- and wear-producing processes, as with rattling gear boxes and heat exchanger tubes.

Vibro-impact problems are often difficult to solve, due to the strong nonlinearities associated with discontinuous or very sudden changes in velocities at impact. In this paper we present a general procedure and several application examples, showing that near-elastic vibro-impact problems can be conveniently analyzed by a discontinuity-reducing transformation of variables, combined with an extended averaging procedure that allows small discontinuities. First- and second-order analytical predictions are derived, and shown to agree to estimated accuracy with results of numerical simulation. We consider only near-elastic vibro-impact, though averaging may be applied also for the inelastic case [2]. Parts of this research have been presented by the authors elsewhere [2-5]; in this paper we collect and expand these results, aiming at a coherent and self-contained presentation, illustration, and test of the procedure.

The classical approach of analyzing vibro-impact problems is *stitching*, i.e. integrating motions between impacts, and using kinematic impact conditions to switch between time intervals of solution [6]. For numerical simulation this may be simple and effective, with appropriate numerical algorithms. However, for obtaining analytical solutions the method is elaborate, and possible only for the simplest systems – and any additional non-linearity makes it very difficult to apply. Furthermore, for typical applications it is not necessary to obtain solutions at the level of detail provided by exact methods. Of more interest may be

* Corresponding author. *E-mail address:* jjt@mek.dtu.dk (J.J. Thomsen).

condensed measures such as oscillation frequencies, stationary amplitudes, and the stability of motions.

Thus, for vibro-impact problems approximate methods are necessary and useful. Among these are the methods of *harmonic linearization* [1], *averaging* [7-9], and *direct separation of motions* [10], each with their particular strengths. In particular the method of harmonic linearization, as introduced by Babitsky [1] in the 1960s, has been used successfully to solve many vibro-impact problems. This approach is convenient in use, but mathematically not well supported; results need careful validation by e.g. numerical simulation, in particular for systems operating away from resonance. Also, harmonic linearization does not distinguish between different dynamical regimes, i.e. the variety of impact oscillations is not captured.

The approach suggested in this paper – discontinuous transformation combined with extended averaging – is mathematically supported by a theorem [2,3] similar to the standard averaging theorem [11], thus providing estimates of the accuracy of approximation, and a systematic procedure for increasing the accuracy to any desired level. By contrast to harmonic linearisation, it assumes a kinematic rather than a kinetic impact formulation. Compared to classical stitching, it works even in the presence of additional nonlinearities, and provides analytical solutions valid at all times, i.e. free of switching conditions. Compared to the averaging approach described by Ivanov [9], the discontinuous transformations need not to eliminate the impacts completely; this implies they are considerably easier to set up and interpret.

The purpose of this paper is to demonstrate the applicability and accuracy of a method for analyzing vibro-impact problems. Thus we attempt describing the method without unnecessary mathematical complication, and to exemplify its use through a range of different applications. The mathematical models used with these examples are chosen for their simplicity and common appearance in applied mechanics; we are not concerned with the accuracy of these models, but only with the accuracy of the method we suggest for analyzing them. Thus we check the accuracy only against numerical simulation of each model, but not against other models or experimental results. Also, aiming at showing several examples, for each example we focus on the key steps in using the proposed method, check its accuracy, and demonstrate the usefulness of having simple analytical results for understanding system behavior – but do not dwell to use the results any further, to examine system behavior more thoroughly.

Section 2 illustrates in a simple setting the basic idea of employing an unfolding transformation to eliminate discontinuities for purely elastic vibro-impact systems. With inelastic impacts such transformations will not eliminate the discontinuities, but for near-elastic impacts they will be reduced to a small value; Thus Section 3 shows how to apply asymptotic first-order averaging for general systems of ordinary differential equations containing small discontinuities. Section 4 presents four application examples, where discontinuous unfolding transformation and averaging are combined, resulting in approximate analytical expressions for key properties such as oscillation amplitudes and frequencies. Section 5 extends the general discontinuous averaging procedure to second order, and presents an application example illustrating the increased accuracy and computational burden, as compared to first-order analysis. Section 6 concludes that discontinuous transformations combined with averaging seems applicable for analyzing a range of vibro-impact problems, and that its potentials could be examined further and compared more systematically to alternative methods.

2. Basic idea of the unfolding discontinuous transformation

Assuming purely elastic impacts, the motions of the harmonic oscillator in Fig. 1(a), bouncing against a rigid stop at $s = 0$, are governed by:

$$\begin{aligned} \ddot{s} + s &= 0 \quad \text{for } s > 0 \\ s_+ &= s_- \quad \text{and } \dot{s}_+ = -\dot{s}_- \quad \text{for } s = 0, \end{aligned} \quad (1)$$

where overdots denote differentiation with respect to time t , and subscripts plus and minus indicate states immediately before and after impact, respectively. The general solution is:

$$s(t) = A|\sin(t + \theta)|, \quad (2)$$

which is shown in Fig. 1(b) (solid line) for initial conditions corresponding to $(A, \theta) = (1, 0)$; it is nothing but a folded sine function. But this in turn means that the discontinuity in (1) can be removed by a discontinuous transformation:

$$s = |z|; \quad z_- z_+ < 0, \quad (3)$$

where the inequality condition implies that the new variable $z(t)$ changes sign at every impact; this removes the non-uniqueness of the transformation due to $|z|$ in the first equation. Inserting (3) into (1), the system transforms into:

$$\begin{aligned} \ddot{z} + z &= 0, \quad z \neq 0 \\ z_+ &= z_- \quad \text{and } \dot{z}_+ = \dot{z}_-, \quad z = 0, \end{aligned} \quad (4)$$

where the second line is given only to emphasize that the transformed system is now continuous at $z=0$; This also appears from the graph of $z(t)$ in Fig. 1(b) (dashed line), where the ‘unfolding’ or mirroring of every other oscillation of $s(t)$ due to (3) is seen to eliminate the discontinuity at zero. Hence the transformation (3) turns (1) into a simple linear oscillator equation, with solution $z = A\sin(t + \theta)$, corresponding to $s = |z| = A|\sin(t + \theta)|$.

Supposing we did not know the exact solution (2), it could be easily derived by first using the discontinuous transformation (3), then solve the transformed system for z , and finally back-transform to obtain s . Even if impacts were not purely elastic, and others sources of energy dissipation or, energy input, and nonlinearities were present, a transformation similar to (3) might be used to eliminate or reduce the discontinuity of the original system.

In many cases relevant for applications, a system so transformed is weakly nonlinear, and contain small discontinuities. Weak nonlinearities can be handled by perturbation methods such as averaging, but even small discontinuities create obstacles for this. Next we describe how to use averaging for systems with small discontinuities.

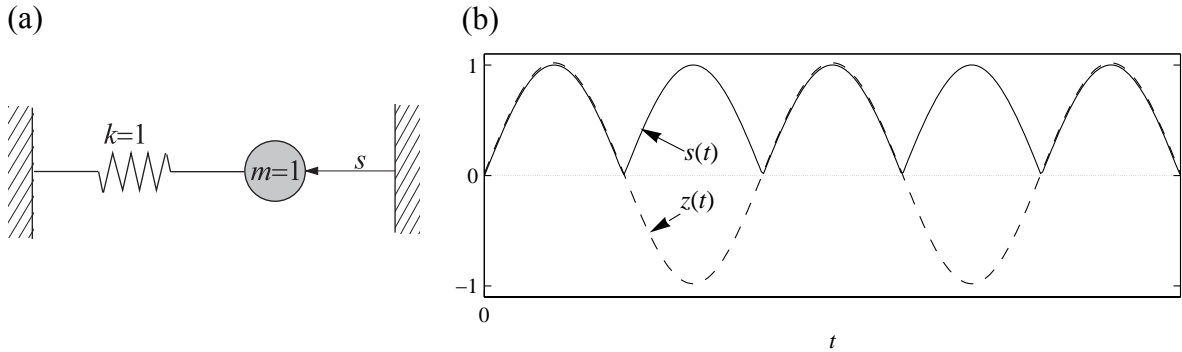


Fig. 1. (a) Harmonic oscillator with a stop. (b) A solution $s(t)$ to (1) (in solid line), and its unfolding $z(t)$ (dashed) as given by the transformation (3).

3. Averaging for vibro-impact systems: General procedure

3.1. Introduction

Common perturbation methods such as averaging [2,12], multiple scales [13,14], harmonic linearization [1], and direct separation of motions [2,10,14] all have difficulties in handling discontinuities such as occur with vibro-impact systems. Typically the coordinates of the impacting objects remain continuous, while the discontinuous change of velocities during impact may be of the order of magnitude of the velocities themselves. An effective approach, which enables the application of averaging to systems with impacts, works by eliminating or reducing the discontinuity from the equations by employing a variable transformation that contains or unfolds the essential discontinuity, as was illustrated for a simple case in Section 2. This idea was suggested by Zhuravlev [8,15-17], and developed for different applications in e.g. [5,9,18-22]. The original objective was to eliminate the discontinuity completely and to apply standard averaging. This is quite successful for perfectly elastic impacts, but in the case of even small energy dissipation during impacts, it becomes difficult to find suitable transformations that seems reasonably simple and with a clear physical interpretation. This seems to impede general use of discontinuity-removing transformations.

However, it is actually not necessary to eliminate the discontinuities completely, but only to reduce them to a sufficiently small level, comparable to other sources of energy dissipation, and to generalize the averaging technique for that case. This combination – of a discontinuity-reducing transformation and generalized averaging – leads to an efficient approach for asymptotic analysis of impacting oscillators, as will be described below and exemplified in the following sections.

3.2. Standard averaging (for smooth systems)

Standard averaging applies to systems of the form:

$$\frac{d\mathbf{x}}{d\varphi} = \varepsilon \mathbf{f}(\varphi, \mathbf{x}), \quad (5)$$

where $\mathbf{x}(\varphi) \in D \subset R^n$ and $\varepsilon \ll 1$ is a small parameter. According to the averaging theorem [11], if \mathbf{f} is 2π -periodic (but not necessarily continuous) in φ and bounded and Lipschitz-continuous in \mathbf{x} on D , then on the scale $\varphi \leq O(1/\varepsilon)$, \mathbf{x} is asymptotically close to the solution \mathbf{x}_1 of the averaged system:

$$\frac{d\mathbf{x}_1}{d\varphi} = \varepsilon \langle \mathbf{f}(\varphi, \mathbf{x}_1) \rangle, \quad (6)$$

where $\langle \cdot \rangle$ denotes averaging over φ :

$$\langle g(\varphi) \rangle_\varphi = \frac{1}{2\pi} \int_0^{2\pi} g(\varphi) d\varphi. \quad (7)$$

For application of the method to be described below, it is important to recall that a function $\mathbf{f}(\mathbf{x}, \varphi)$, $\mathbf{x}(\varphi) \in D \subset R^n$, is bounded and Lipschitz-continuous in \mathbf{x} on D if and only if non-negative constants M_f and λ_f exist such that, for all $(\mathbf{x}_1, \mathbf{x}_2) \in D$:

$$\|\mathbf{f}(\mathbf{x}, \varphi)\| \leq M_f \quad \text{and} \quad \|\mathbf{f}(\mathbf{x}_1, \varphi) - \mathbf{f}(\mathbf{x}_2, \varphi)\| \leq \lambda_x \|\mathbf{x}_1 - \mathbf{x}_2\|. \quad (8)$$

In other words, a Lipschitz-continuous function $\mathbf{f}(\mathbf{x}, \varphi)$ is limited in how fast it can change with \mathbf{x} : The slope of a line (in R^n) joining any two points on the graph (in R^n) of the function

will never exceed its Lipschitz-constant λ .

3.3. Generalized first-order averaging (for discontinuous systems)

For vibro-impact problems formulated with kinematic impact conditions, the inherent discontinuities in velocity preclude using standard averaging. However, a special form of the averaging theorem can be proved [8], that holds for systems with *small* (i.e. $O(\varepsilon)$) discontinuities in the state variables, that is, instead of (5):

$$\begin{aligned} \frac{d\mathbf{x}}{d\varphi} &= \varepsilon \mathbf{f}(\mathbf{x}, \varphi) \text{ for } \varphi \neq j\pi, j=0,1,\dots, \mathbf{x}(\varphi) \in D \subset R^n, \varepsilon \ll 1 \\ \mathbf{x}_+ - \mathbf{x}_- &= \varepsilon \mathbf{g}(\mathbf{x}_-) \text{ for } \varphi = j\pi, \end{aligned} \quad (9)$$

where \mathbf{f} is 2π -periodic (not necessarily continuous) in φ , \mathbf{f} and \mathbf{g} are bounded and Lipschitz-continuous in \mathbf{x} on $\mathbf{x} \in D \subset R^n$, and \mathbf{x}_- and \mathbf{x}_+ are the states \mathbf{x} immediately before and after the j 'th impact, corresponding to the passage of φ through the value $j\pi$. For that case the averaged system becomes, instead of (6) ([2,3,8] and Section 5.1):

$$\frac{d\mathbf{x}_1}{d\varphi} = \varepsilon \left(\langle \mathbf{f}(\mathbf{x}_1, \varphi) \rangle_\varphi + \pi^{-1} \mathbf{g}(\mathbf{x}_1) \right), \quad (10)$$

where the subscript 1 indicates the first level of approximation to \mathbf{x} , i.e. $\mathbf{x} = \mathbf{x}_1 + \varepsilon \mathbf{x}_2 + O(\varepsilon^2)$, so that the error $\|\mathbf{x}_1(t) - \mathbf{x}(t)\|$ is $O(\varepsilon)$ on the time-scale $1/\varepsilon$. The averaged motions \mathbf{x}_1 may themselves be determined at different levels of accuracy, i.e. $\mathbf{x}_1 = \mathbf{x}_{11} + \varepsilon \mathbf{x}_{12} + O(\varepsilon^2)$, of which (10) gives the first order approximation \mathbf{x}_{11} , while the second-order approximation(s) \mathbf{x}_{12} (and \mathbf{x}_2) are derived in Section 5.

To transform vibro-impact problems into the form (9) may be non-trivial, in particular since for near-elastic vibro-impact the discontinuity in velocity is not small. At least two transformations are then required: One for transforming large discontinuities into small ones, and another one for transforming the impact-free part of the equations of motion into the form of the first equation in (9). Below we illustrate how this can be accomplished for specific examples of vibro-impact systems.

4. Discontinuous transformation and averaging combined: Examples

4.1. Harmonic oscillator with viscous damping and near-elastic impacts against a stop

Consider the system in Fig. 2, which is an extension of the harmonic oscillator with a stop in Section 2. Here we assume inelastic impacts with a coefficient of restitution R slightly less than unity, linear viscous damping in-between impacts with small coefficient β , and a stop situated a small distance Δ away from the equilibrium (without stop) of the spring at $s = 0$. The motions are governed by:

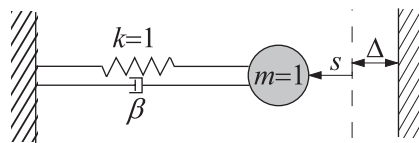


Fig. 2. Harmonic oscillator with near-elastic impacts, viscous damping, and a stop offset from the equilibrium of the spring.

$$\begin{aligned} \ddot{s} + 2\beta\dot{s} + s &= 0 \quad \text{for } s > -\Delta \\ s_+ &= s_-; \quad \dot{s}_+ = -R\dot{s}_- \quad \text{for } s = -\Delta, \end{aligned} \quad (11)$$

with $s = s(t)$, given initial conditions $s(0)$ and $\dot{s}(0)$, and:

$$0 < \beta \ll 1; \quad 0 < (1-R) \ll 1; \quad |\Delta| \ll 1. \quad (12)$$

The unfolding transformation (3) can be used also here, slightly modified:

$$s = |z| - \Delta, \quad z_- z_+ < 0. \quad (13)$$

Inserting this into (11) gives a transformed system in the new dependent variable z :

$$\begin{aligned} \ddot{z} + 2\beta\dot{z} + z &= \Delta \operatorname{sgn} z, \quad z \neq 0 \\ z_+ - z_- &= 0; \quad \dot{z}_+ - \dot{z}_- = -(1-R)\dot{z}_-, \quad z = 0. \end{aligned} \quad (14)$$

The main difference between (11) and (14) is, that in (14) the discontinuous jump in velocity at impact ($s = -\Delta$ or $z = 0$) has been reduced to a small value (proportional to $1-R$), while a small nonlinearity (proportional to Δ) has emerged in the equation of motion valid in-between impacts ($z \neq 0$). Though (14) is still nonlinear, it is only weakly so, which means that perturbation methods can be applied to calculate approximate solutions as follows:

Considering terms in (14) having small coefficients as perturbations, the unperturbed system corresponding to (14) is a linear undamped and unforced harmonic oscillator. This means that the method of averaging can be used, after having applied a standard van der Pol transformation (e.g. [2,11-13]):

$$z = A \sin \psi; \quad \dot{z} = A \cos \psi; \quad \psi = t + \theta, \quad (15)$$

from which directly follows:

$$A\dot{\theta} = -\dot{A} \tan \psi; \quad \dot{\psi} = 1 + \dot{\theta}; \quad \ddot{z} = \dot{A}/\cos \psi - A \sin \psi. \quad (16)$$

where $A=A(t) > 0$ and $\theta=\theta(t)$ denote the slowly changing amplitude and phase, respectively. Inserting (15) and (16) into (14) gives the following system in the new dependent variables A and θ :

$$\left. \begin{aligned} \dot{A} &= -2\beta A \cos^2 \psi + \Delta \cos \psi \operatorname{sgn}(\sin \psi) \\ \dot{\theta} &= 2\beta \sin \psi \cos \psi - \frac{\Delta}{A} |\sin \psi| \end{aligned} \right\}, \quad \psi \neq j\pi, \quad j=0,1,\dots \quad (17)$$

$$\left. \begin{aligned} A_+ - A_- &= -(1-R)A_- \\ \theta_+ - \theta_- &= 0 \end{aligned} \right\}, \quad \psi = j\pi,$$

where impacts occur at $\psi = j\pi$. With small parameters as assumed in (12), and assuming also $A \gg |\Delta|$, we note from (17) that \dot{A} and $\dot{\theta}$ are $O(\Delta, \beta)$, so that:

$$\begin{aligned} \frac{dA}{d\psi} &= \frac{\dot{A}}{\dot{\psi}} = \frac{\dot{A}}{1+\dot{\theta}} = \dot{A}(1+O(\dot{\theta})) = \dot{A} + O(\dot{A})O(\dot{\theta}) = \dot{A} + O((\Delta, \beta)^2) \\ \frac{d\theta}{d\psi} &= \frac{\dot{\theta}}{\dot{\psi}} = \frac{\dot{\theta}}{1+\dot{\theta}} = \dot{\theta}(1+O(\dot{\theta})) = \dot{\theta} + O(\dot{\theta})O(\dot{\theta}) = \dot{\theta} + O((\Delta, \beta)^2) \end{aligned} \quad (18)$$

Thus, to first order of accuracy of the small parameters, we can replace \dot{A} and $\dot{\theta}$ with $dA/d\psi$ and $d\theta/d\psi$, respectively. Then (17) has the general form (9) with:

$$\begin{aligned} \varphi = \psi; \quad \mathbf{x}(\varphi) &= \begin{Bmatrix} A(\psi) \\ \theta(\psi) \end{Bmatrix}; \quad \varepsilon \mathbf{g}(\mathbf{x}) = \begin{Bmatrix} -(1-R)A \\ 0 \end{Bmatrix}; \\ \varepsilon \mathbf{f}(\mathbf{x}, \varphi) &= \begin{Bmatrix} -2\beta A \cos^2 \psi + \Delta \cos \psi \operatorname{sgn}(\sin \psi) \\ 2\beta \sin \psi \cos \psi - (\Delta/A) |\sin \psi| \end{Bmatrix}. \end{aligned} \quad (19)$$

The condition under (9), that \mathbf{f} and \mathbf{g} should be bounded and Lipschitz-continuous in $(A, \theta) \in D \subset \mathbb{R}^2$, is seen to be fulfilled when Δ/A is bounded and Lipschitz-continuous in A ; this holds true under the already stated assumption $A \gg |\Delta|$.

With the conditions fulfilled, application of (10) with (7) to (17) gives the averaged system

$$\begin{aligned} \dot{A}_1 &= -\tilde{\beta} A_1; \quad \tilde{\beta} = \beta + \frac{1-R}{\pi} \\ \dot{\theta}_1 &= -\frac{2\Delta}{\pi A_1}. \end{aligned} \quad (20)$$

where the subscript 1 indicates a first-order approximate solution, asymptotically valid under assumptions (12), and the effective damping constant $\tilde{\beta}$ is seen to integrate the two dissipative effects present: inelastic restitution during impacts, and viscous damping in-between impacts. This linear system can readily be integrated to give:

$$\begin{aligned} A_1 &= C_1 e^{-\tilde{\beta} t}, \quad C_1 > 0 \\ \theta_1 &= -\frac{2\Delta}{\pi C_1 \tilde{\beta}} e^{\tilde{\beta} t} + C_2, \end{aligned} \quad (21)$$

where the constants C_1 and C_2 are determined by initial conditions. Back-substituting this into (15) and (13) gives the approximate solution s_1 for the original variable s :

$$\begin{aligned} s_1 &= C_1 e^{-\tilde{\beta} t} \left| \sin \left(t - \frac{2\Delta}{\pi C_1 \tilde{\beta}} e^{\tilde{\beta} t} + C_2 \right) \right| - \Delta, \quad 0 < t < t_*, \\ t_* &= O \left(\min \left\{ \tilde{\beta}^{-1}, |\Delta|^{-1}, \tilde{\beta}^{-1} \ln \left(C_1 |\Delta|^{-1} \right) \right\} \right), \end{aligned} \quad (22)$$

where the time-horizon t_* ensures the error in s_1 to be of the same magnitude order as the small parameters (*cf.* the error estimate under (10)), and that $A_1 > |\Delta|$ (to ensure boundedness and Lipschitz continuity, *cf.* the remark under (19)).

Fig. 3 compares this approximate solution with results of numerical simulation of the original equation of motion (11) (using the built-in MATLAB-function *ode23* with impacts handled by the *event function* feature), for parameters as indicated in the figure legend. The equilibrium mass-to-stop distance Δ is positive for the left figures (a,c) (corresponding to a unilateral clearance), and negative for the right figures (b,d) (i.e. the mass is pre-compressed against the stop). For the upper figs. (a,b) the small parameters are of the order $\varepsilon = 0.01$, and there is no discernible difference between approximate and simulated response. For the lower figs. (c,d) the small parameters are 10 times larger, and at the end $t = t_*$ (*cf.* (22)) of the time series there are visible discrepancies of order magnitude 0.1 between the approximate and the simulated response. These findings are consistent with the accuracy estimate given under (10), according to which the error at $t = t_* = O(\tilde{\beta}^{-1}, \Delta^{-1})$ is of the same magnitude order as the small parameters, i.e. 0.01 for figs. (a,b), and 0.1 for figs. (c,d). This highlights the asymptotic nature of the analytical prediction (22), which implies that the quality of predictions decline as the assumption of small parameters (and Lipschitz continuity) fails to hold.

Note however, that the quality of predictions at a given level of parameter-smallness can be systematically improved by using higher order approximations (*cf.* Section 5).

It should be recalled that the small parameters should be “small” as compared to the oscillation amplitude A , *cf.* the discussion below (19). When $|s|$ drops below $|\Delta|$, which occurs for $t \gg t_*$, then the parameters cannot longer be considered “small”, and (22) will not provide a good approximation. This holds even for $\Delta > 0$, where $|s| < |\Delta|$ implies the mass does not hit the stop, and the system becomes linear with a simple exponentially decaying harmonic solution: The nonlinear asymptotic solution (22) is incapable of reproducing this.

We have demonstrated how a discontinuous transformation followed by averaging can provide simple, analytical predictions of the response of a strongly nonlinear vibro-impact system, provided the dissipation is weak and the stop is situated near the equilibrium. Here the system was considered linear in-between impacts, but this is not necessary: Weak nonlinearities could be added to (11) without causing additional complications in the procedure; this is illustrated in Sections 4.3, 4.4, and 5.2.

4.2. Mass in a clearance

The motions of a free mass in a clearance 2Δ (Fig. 4) is governed by:

$$\begin{aligned} \ddot{s} &= 0 \quad \text{for } |s| < \Delta \\ s_+ &= s_-; \quad \dot{s}_+ = -R\dot{s}_- \quad \text{for } |s| = \Delta, \end{aligned} \quad (23)$$

where the impacts at $|s| = \Delta$ are assumed to be near-elastic, $0 < (1-R) \ll 1$, while Δ can be arbitrarily large. There will be discontinuous changes in velocity at the times of impact. To set up a suitable transformation for eliminating or reducing these, we first note that for purely elastic impacts ($R = 1$) the speed $|\dot{s}|$ remains unchanged between all impacts, i.e. the coordinate s will trace out a regular zigzag line in time. Such a folded line can be described by standard trigonometric functions, for example:

$$\Pi(z) = \arcsin(\sin z), \quad (24)$$

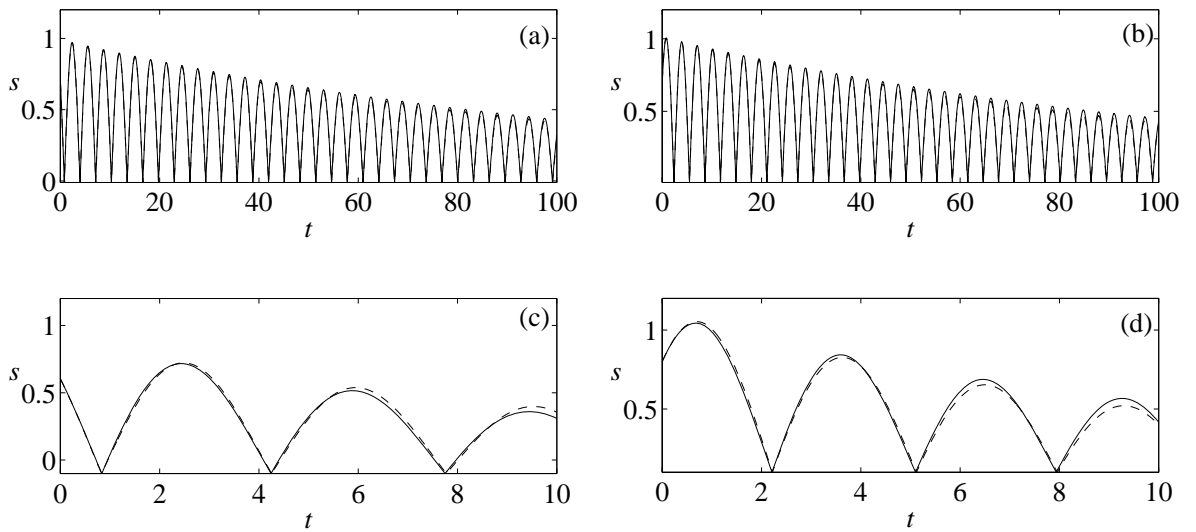


Fig. 3. Impact oscillator position $s(t)$, $t \in [0; t_*]$, as obtained by the approximate analytical prediction (22) (in solid line), and by numerical simulation of the original equation of motion (11) (dashed line), for initial conditions corresponding to $(C_1, C_2) = (1, 0)$ Parameter values $(\Delta, 1-R, \beta)$: In (a): $(\varepsilon, \varepsilon, \varepsilon)$, in (b): $(-\varepsilon, \varepsilon, \varepsilon)$, in (c): $(10\varepsilon, 10\varepsilon, 10\varepsilon)$, in (d): $(-10\varepsilon, 10\varepsilon, 10\varepsilon)$, where $\varepsilon = 0.01$.

which is depicted in Fig. 5(a). Thus, if a curve $z(t)$ is a straight line, then $\Pi(z(t))$ is a zigzag line, 2π -periodic in z (but not necessarily in t). Consequently, if $z(t)$ is “almost” a straight line, i.e. $z(t) = c_0 + c_1 t + \varepsilon(t)$, $\varepsilon \ll 1$, then $\Pi(z(t))$ can be considered a slightly perturbed zigzag line. Conversely, if $\Pi(z(t))$ is (close to) a periodic zigzag line, then $z(t)$ is (close to) a straight line, i.e.: all the “zags” of $\Pi(z(t))$ are mirrored about a line parallel to the time axis, to create an unfolded line that is (close to) straight.

Now, when $R = 1$, the variable s in (23) describes a zigzag line in time with period $4\Delta/|\dot{s}|$, where $|\dot{s}|$ is the constant speed. With near-elastic impacts, $0 < 1 - R \ll 1$, $|\dot{s}|$ will decrease at bit at every impact, and so will the slopes of the zigs and zags of $s(t)$, which becomes a close-to-periodic zigzag line. Thus, as an unfolding transformation for s we may use:

$$s = \frac{2\Delta}{\pi} \Pi(z), \quad (25)$$

which was suggested by Zhuravlev and Klimov [8] for $R=1$, but here we use it even for $R \approx 1$. From (24) and (25) it follows that:

$$\dot{s} = \frac{2\Delta}{\pi} M(z) \dot{z}, \quad \ddot{s} = \frac{2\Delta}{\pi} (M'(z) \dot{z} + M(z) \ddot{z}) \quad \text{for } z \neq \frac{\pi}{2} + j\pi, \quad j = 0, 1, \dots, \quad (26)$$

where $M(z) = d\Pi/dz = \text{sgn}(\cos z)$. Then, with (24)-(26), the system (23) transforms into:

$$\begin{aligned} \ddot{z} &= 0, \quad z \neq \frac{\pi}{2} + j\pi, \quad j = 0, 1, \dots \\ z_+ &= z_-, \quad \dot{z}_+ - \dot{z}_- = -(1-R)\dot{z}_-, \quad z = \frac{\pi}{2} + j\pi. \end{aligned} \quad (27)$$

where it appears that the discontinuity in the velocity \dot{z} of the new dependent variable has been reduced to a small value, proportional to $(1-R)$. This also appears from Fig. 5(b), where $z(t)$ describes a polygon with small angles between the straight line segments, i.e. the changes in slope of $z(t)$ are much smaller than those of $s(t)$.

To transform (27) further into the general form (9), we first reduce to the required first-order form by introducing a new dependent variable $v = \dot{z}$, so that (27) becomes:

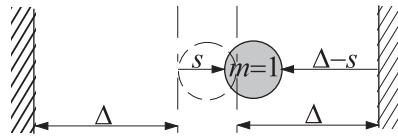


Fig. 4. Simple impact oscillator: Mass in a clearance

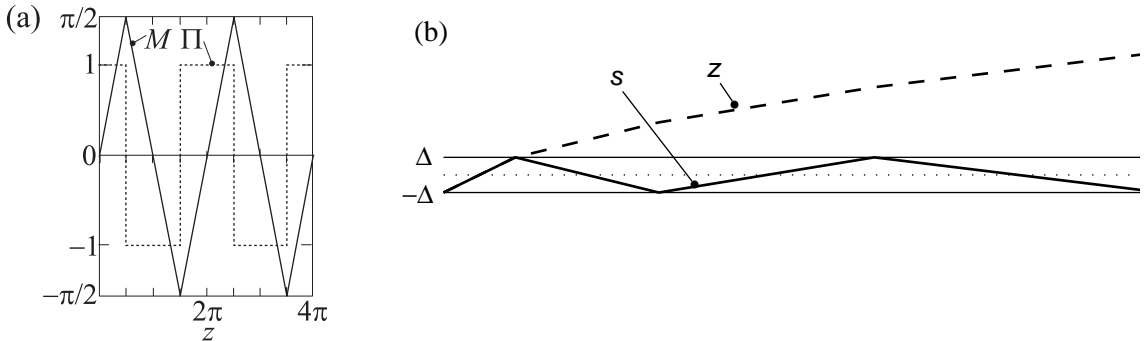


Fig. 5. (a) Function $\Pi(z)$ in (24) and its derivative $M(z)$; (b) Motions $s(t)$ of the mass in a clearance for $0 < 1 - R \ll 1$, and its unfolding $z(t)$ as given by the transformation (25)

$$\left. \begin{aligned} \dot{z} &= v \\ \dot{v} &= 0 \end{aligned} \right\}, \quad z \neq \frac{\pi}{2} + j\pi, \quad j = 0, 1, \dots \quad (28)$$

$$\left. \begin{aligned} z_+ - z_- &= 0 \\ v_+ - v_- &= -(1-R)v_- \end{aligned} \right\}, \quad z = \frac{\pi}{2} + j\pi,$$

or, eliminating time as the independent by dividing the second equation with the first:

$$\frac{dv}{dz} = 0, \quad z \neq \frac{\pi}{2} + j\pi \quad (29)$$

$$v_+ - v_- = -(1-R)v_-, \quad z = \frac{\pi}{2} + j\pi,$$

where z now takes the role of the independent variable. This system has the general form (9), and can thus be averaged using (10) into:

$$\frac{dv_1}{dz_1} = -\frac{1-R}{\pi}v_1; \quad v_1 = \frac{dz_1}{dt}, \quad (30)$$

which is a linear system with solution:

$$z_1 = \frac{\pi}{1-R} \ln(C_1 t + C_2); \quad v_1 = \frac{\pi}{1-R} \frac{C_1}{C_1 t + C_2}, \quad (31)$$

where the constants $C_1 > 0$ and C_2 are determined by initial conditions. The corresponding motion of the original variable $s(t)$ is then, by (25):

$$s = \frac{2\Delta}{\pi} \Pi \left(\frac{\pi}{1-R} \ln(C_1 t + C_2) \right). \quad (32)$$

Fig. 6 compares results of using the approximate first-order prediction (32) to results of numerical simulations of the original system (23); as appears there is no discernible difference in results for the position variable $s(t)$. For the velocity $\dot{s}(t)$ the difference is small but clear, and in fact very illustrative of the effect of discontinuous averaging of systems with near-elastic impacts: The vertical lines for \dot{s} in Fig. 6 correspond to impacts, where the velocity changes sign and its magnitude drops the small value $1-R$. The horizontal lines in the numerical solution (dashed) correspond to time intervals of free flight with constant velocity. In the approximate solution, by contrast, there is no change in velocity magnitude after impacts; instead the change is distributed over the time interval between impacts, keeping the average energy loss the same as for the numerical solution. Thus the inaccuracy of the approximate solution for the velocity \dot{s} is of the order of magnitude of the small parameters, while the inaccuracy in position s is even smaller.

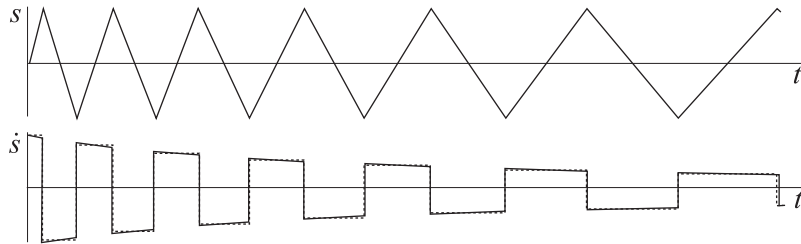


Fig. 6. Position $s(t)$ and velocity $\dot{s}(t)$ of a mass in a clearance 2Δ , as predicted by the approximate expression (32) (solid line), and numerical simulation of (23) (dashed line); $R = 0.9$.

4.3. Self-excited friction oscillator with a one-sided stop

Fig. 7(a) shows the classical ‘mass on moving belt’ model [23], though extended with a stop at the right, which restricts motions to $s < \Delta$ (the left stop is ignored in this section). Without stop(s) this system is often used for illustrating friction-induced oscillations; for example [24] uses averaging to derive stationary amplitudes for pure slip and stick-slip oscillations. With one- or two-sided stops, it models rubbing objects with slipping parts, e.g., loosely mounted brake pads.

A typical nondimensional model formulation is:

$$\begin{aligned} \ddot{s} + s &= -h(\dot{s}) \quad \text{for } s < \Delta; \quad h(\dot{s}) = h_1 \dot{s} + h_2 \dot{s}^2 + h_3 \dot{s}^3, \quad \dot{s} < v_b \\ s_+ &= s_-, \quad \dot{s}_+ = -R\dot{s}_- \quad \text{for } s = \Delta, \end{aligned} \quad (33)$$

where $s(t)$ is the displacement of the mass from the static equilibrium $s_0 = \mu(-v_b)$ at belt speed v_b , the friction law is a cubic Stribeck model with friction coefficient $\mu(v_r) = \mu_s \text{sgn}(v_r) - k_1 v_r + k_3 v_r^3$ depending on relative interface velocity v_r ([24,25] and Fig. 7(b)), μ_s is the static coefficient of friction, k_1 the slope of the friction-velocity curve at zero relative velocity, k_3 the coefficient governing increased friction at higher velocities, $h_1 = 2\beta - k_1 + 3k_3 v_b^2 < 0$, $h_2 = -3k_3 v_b$, $h_3 = k_3$, R is the coefficient of impact restitution, and β the linear viscous damping ratio. Of interest here is the effect of impacts, so $\dot{s} < v_b$ is assumed to avoid unnecessary complications connected with sticking motions ([24] consider stick-slip).

Assuming weak dissipation, the parameters h_1 , h_2 , and h_3 are small. In addition we assume near-elastic impacts, and a small distance from the equilibrium of the unstrained spring, i.e.:

$$0 < (1 - R) \ll 1; \quad |h_{1,2,3}| \ll 1; \quad |\Delta| \ll 1. \quad (34)$$

To turn (33) into the form (9), we repeat the procedure from Section 4.1, and even start with the same discontinuous transformation (13), though with a shift in sign since the stop is now situated $s = +\Delta$:

$$s = \Delta - |z|; \quad z_+ z_- < 0. \quad (35)$$

Then, in the z -variable, every other oscillation of s and \dot{s} will be mirrored, so that if $R=1$ the velocity-discontinuity at impact is eliminated, while for near-elastic impacts $0 < (1-R) \ll 1$ the discontinuity will be small, as illustrated in Fig. 8. Inserting (35) into (33), the transformed system becomes:

$$\begin{aligned} \ddot{z} + z &= \Delta \text{sgn } z - h_1 \dot{z} + h_2 \dot{z}^2 \text{sgn } z - h_3 \dot{z}^3 \quad \text{for } z \neq 0, \quad |\dot{z}| < v_b \\ \dot{z}_+ - \dot{z}_- &= -(1 - R)\dot{z}_- \quad \text{for } z = 0. \end{aligned} \quad (36)$$

Next, to turn (36) further into the form (9), we note that the first equation in (36) is quasi-

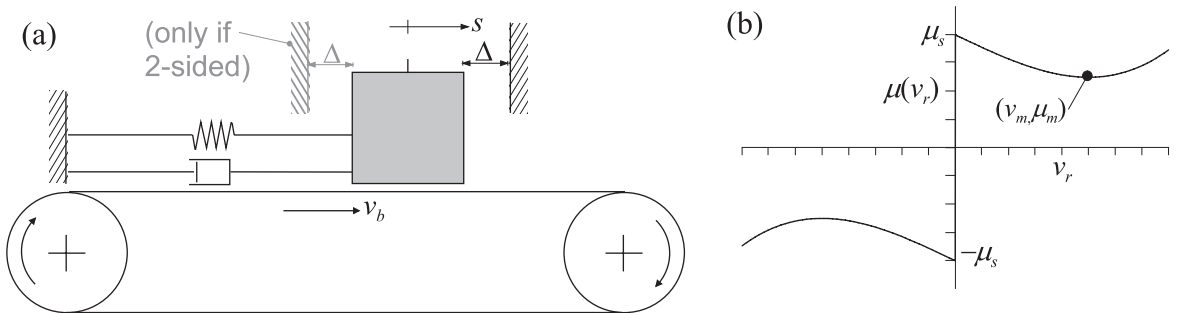


Fig. 7. (a) Self-excited friction-oscillator with one or two stops; (b) Friction coefficient μ as a function of relative interface velocity v_r .

linear, so that the standard van der Pol transformation (15)-(16) can be used again, giving:

$$\left. \begin{aligned} \dot{A} &= (\Delta + h_2 A^2 \cos^2 \psi) \cos \psi \operatorname{sgn}(\sin \psi) \\ &\quad - (h_1 + h_3 A^2 \cos^2 \psi) A \cos^2 \psi \\ \dot{\theta} &= -\left(\frac{\Delta}{A} + h_2 A \cos^2 \psi \right) |\sin \psi| + (h_1 + h_3 A^2 \cos^2 \psi) \cos \psi \sin \psi \end{aligned} \right\}, \quad \psi \neq j\pi, \quad j=0,1,\dots \quad (37)$$

$$\left. \begin{aligned} A_+ - A_- &= -(1-R)A_- \\ \theta_+ - \theta_- &= 0, \quad \psi = j\pi \end{aligned} \right\}, \quad \psi = j\pi,$$

Under assumptions (34) and $A \gg |\Delta|$ we find, using order analysis as in (18), that $dA/d\psi = \dot{A} + O((\Delta, h_{1,2,3})^2)$ and $d\theta/d\psi = \dot{\theta} + O((\Delta, h_{1,2,3})^2)$, so that to first order of accuracy of the small parameters, we can replace \dot{A} and $\dot{\theta}$ with $dA/d\psi$ and $d\theta/d\psi$, respectively. Then (37) has the general form (9), and (10) can be used to calculate the averaged system:

$$\begin{aligned} \dot{A}_1 &= -\hat{\beta} A_1 - \frac{3h_3 A_1^3}{8}; \quad \hat{\beta} = \frac{h_1}{2} + \frac{1-R}{\pi} \\ \dot{\theta}_1 &= -\frac{2}{\pi} \left(\frac{\Delta}{A_1} + \frac{h_2 A_1}{3} \right). \end{aligned} \quad (38)$$

This system is rather similar to (20) for the viscously damped simple impact oscillator, though, with the important difference that in (38) the linear ‘‘damping’’ parameter $\hat{\beta}$ can be also negative (if h_1 is sufficiently negative, *cf.* the definition of h_1 below (33)). In that case energy from the running belt is transferred to the mass and the spring, leading to self-excited oscillations that may be stabilized by nonlinearities such as the h_3 -term.

Though the system (38) is (weakly) nonlinear, we can easily determine the stationary solutions, which are those of primary interest: By (35) and (15) we have:

$$s_1 = \Delta - A_1 |\sin(t + \theta)|, \quad (39)$$

and thus constant-amplitude solutions can be identified by letting $\dot{A}_1 = 0$ in (38). This gives a trivial solution $A_1 = 0$ (where the mass does not move), and a non-trivial solution $A_1 = A_{1\infty}$ corresponding to stationary oscillations,

$$A_{1\infty} = \sqrt{\frac{8\hat{\beta}}{3h_3}}. \quad (40)$$

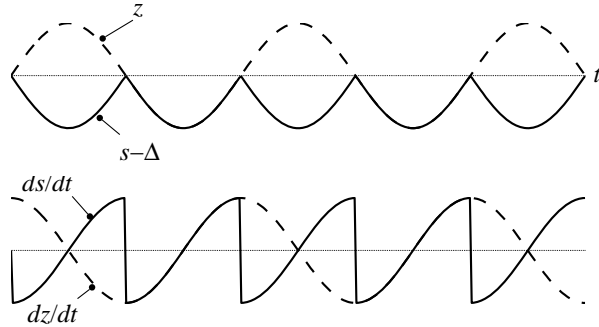


Fig. 8. Motions of a friction-oscillator with a near-elastic stop. In the transformed variable z , the discontinuity in velocity dz/dt is small, while for the original variable s the discontinuity in ds/dt is large.

This solution is stable (i.e. $\partial \dot{A}_1 / \partial A_1 < 0$ from (38) with $A_1 = A_{1\infty}$) only when it exists, i.e. when $\hat{\beta} < 0$ for $h_3 > 0$, and in that case the trivial solution $A_1 = 0$ is unstable. In (40) the inelasticity of impacts is present only through the parameter $\hat{\beta}$, which combines the dissipative effects of friction and impact, *cf.* (38). In the absence of impacts $\hat{\beta} = h_1/2$, and expression (40) for the oscillation amplitude reduces to the known expression for the no-stick oscillation amplitude of a cubic friction oscillator [24]. Hence, the effect of near elastic impacts on oscillation amplitude is equivalent to that of linear viscous damping with coefficient $\frac{2}{\pi}(1-R)$, *cf.* (38). Examining this equivalence further, it turns out, that most of the (non-sticking) analytical results derived in [24] for the system without stop also hold for the system with one-sided stop – provided the linear dissipation parameter β is replaced everywhere by the effective viscous damping coefficient $\hat{\beta}$ as defined in (38), and the low-speed slope h_1 of the friction curve is replaced by the effective value $\hat{h}_1 = 2\hat{\beta} - k_1 + 3k_3 v_b^2$.

Substituting (40) into the second equation in (38), and solving the linear equation for θ_1 , one finds:

$$\theta_{1\infty} = \frac{-2}{\pi A_{1\infty}} \left(\Delta + \frac{1}{3} h_2 A_{1\infty}^2 \right) t + \theta_0, \quad (41)$$

so that by (39) the oscillating stationary solution $s_{1\infty}$ can be written:

$$s_{1\infty} = \Delta - A_{1\infty} \left| \sin(\omega_\infty t + \theta_0) \right|; \quad \omega_\infty = 1 - \frac{2}{\pi A_{1\infty}} \left(\Delta + \frac{1}{3} h_2 A_{1\infty}^2 \right), \quad (42)$$

where θ_0 is an arbitrary constant phase, and the oscillation period is π/ω_∞ . This simple expression for the oscillations of the strongly nonlinear vibro-impact problem with friction provides good agreement with numerical simulation, even for larger values of $|1-R|$, as long as Δ is small. Fig. 9 shows an example, with parameters (given in the figure legend) resulting in $\hat{\beta} = -0.0068$ and $A_{1\infty} = 0.60$, and good agreement between the approximation (42) (in solid line) and numerical simulation of the original equation of motion (33) (dashed). With other parameters, the errors (i.e. deviations from numerical simulation), will decrease or increase as the parameters assumed small in (34) becomes smaller or larger, respectively. Also, for fixed parameters, the errors can be reduced by using a more accurate second order analysis, the result of which is shown dotted in Fig. 9, and discussed in detail in Section 5.2.

As appears from (40) and Fig. 10 (solid line), the first-order approximation to the stationary oscillation amplitude $A_{1\infty}$ does not depend on the equilibrium-to-stop distance Δ , while numerical simulation shows a clear increase of $A_{1\infty}$ with Δ (Fig. 10, circles). For small Δ the error resulting from this is $\mathcal{O}(\Delta)$, which is consistent with the error estimate under (10). For larger Δ the accuracy can be improved by using second-order averaging, *cf.* Fig. 10 (dotted line) and Section 5.2.

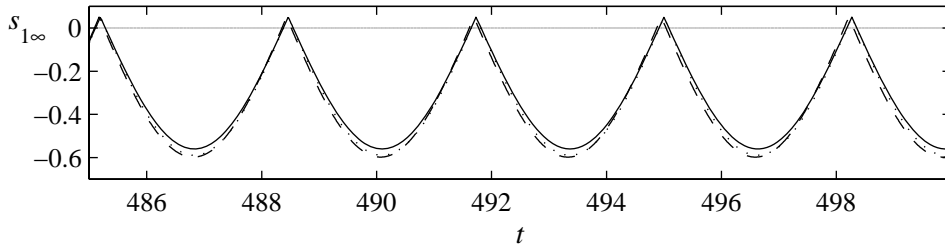


Fig. 9. Friction oscillator displacement $s_{1\infty}$ as a function of time t , comparing the analytic first-order prediction (42) (solid line), the second-order approximation (81) (dotted), and numerical simulation of the original equation of motion (33) (dashed). Parameters: $h_1 = -0.02$, $h_2 = -0.1$, $h_3 = 0.05$, $R = 0.99$, $\Delta = 0.05$.

4.4. Self-excited friction oscillator with a two-sided symmetrical stop

With a two-stop friction-oscillator (Fig. 7(a)), we assume the static equilibrium of the mass on the running belt to be in the middle of the clearance 2Δ , but do not assume this clearance to be small. Motions $s(t)$ are governed by the nondimensional system:

$$\begin{aligned} \ddot{s} + s &= -h(\dot{s}) \quad \text{for } |s| < \Delta; \quad h(\dot{s}) = h_1\dot{s} + h_2\dot{s}^2 + h_3\dot{s}^3, \quad \dot{s} < v_b \\ s_+ &= s_-, \quad \dot{s}_+ = -R\dot{s}_- \quad \text{for } |s| = \Delta, \end{aligned} \quad (43)$$

which differs from the one-stop system (33) only in the impact condition being changed from $s=\Delta$ to $|s|=\Delta$. However, this changes the character of solutions so that the mirror-transformation (35), used for the one-stop system, will not reduce the velocity-discontinuity to a small value. Instead we re-employ the transformation (25), used for the problem of a free mass in a clearance:

$$s = \frac{2\Delta}{\pi} \Pi(z), \quad (44)$$

with Π defined by (24). Inserting this into (43) gives:

$$\begin{aligned} \dot{z} + M(z)\Pi(z) &= -\bar{h}_1\dot{z} - \bar{h}_2\dot{z}^2 M(z) - \bar{h}_3\dot{z}^3, \quad z \neq \frac{\pi}{2} + j\pi, \quad j = 0, 1, \dots \\ \dot{z}_+ - \dot{z}_- &= -(1-R)\dot{z}_-, \quad z = \frac{\pi}{2} + j\pi, \end{aligned} \quad (45)$$

where $\bar{h}_1 = h_1$, $\bar{h}_2 = 2\Delta h_2/\pi$, $\bar{h}_3 = 4\Delta^2 h_3/\pi^2$, and $M(z) = d\Pi/dz$. We assume a small energy input (corresponding to a small negative slope of the friction characteristics), and small energy dissipation due to friction and impact, i.e.:

$$0 < (1-R) \ll 1; \quad |\bar{h}_{1,2,3}| \ll 1; \quad \Delta = O(1). \quad (46)$$

Next we need to transform (45) into the general form (9) applicable for averaging. This time the van der Pol transformation (15) will not do that, since when hitting two stops, motions of the mass cannot be adequately approximated by slowly amplitude- and phase-modulated time-harmonic functions. Instead this we rely on the well-proven general method of transforming weakly nonlinear differential equations into the first-order form appropriate for standard averaging, that is: First solve the unperturbed system, then consider the free constants of this solutions as new time-dependent variables, and finally substitute the solution into the nonlinear equations of motions to obtain the equations governing the slow evolution of these variables. For classical weakly nonlinear oscillators this approach results in the van der Pol transformation (15). Here, to find a workable transformation, we consider the unperturbed system corresponding to (45), which can be written in terms of a potential V :

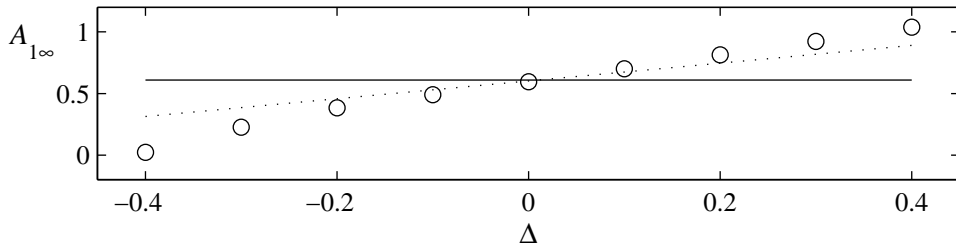


Fig. 10. Stationary amplitude $A_{1\infty}$ as a function of the distance Δ from the (unstable) equilibrium of the mass on a moving belt to the hard stop: The analytic first-order prediction (40) (solid line), the analytical second-order prediction (81) with (85)-(86) (dotted), and numerical simulation of the original equation of motion (33) (circles). Parameters as for Fig. 9.

$$\ddot{z}_0 + \frac{dV}{dz_0} = 0; \quad V(z_0) = \int_0^{z_0} M(\zeta) \Pi(\zeta) d\zeta, \quad (47)$$

where subscript zero indicates unperturbed variables. Multiplying by \dot{z}_0 and integrating over time gives:

$$E = \frac{1}{2} \dot{z}_0^2 + V(z_0) \quad (48)$$

where the potential energy $V(z_0)$ is π -periodic with each period defined by a positive parabola, and the constant of integration E is the mechanical energy of the unperturbed system. This energy is limited by two conditions: First the condition $\dot{z}_0^2 > 0$ with (48) gives $E > V(z_0)$, which implies $E > \max(V(z_0)) = V(\pi/2) = \pi^2/8$, and second we consider only slipping motions, i.e. $\dot{s} < v_b$, which with (44), (48), and $M^2 = 1$ implies $E < \frac{\pi^2}{8} (1 + (v_b/\Delta)^2)$, hence:

$$1 < \frac{8E}{\pi^2} < 1 + (v_b/\Delta)^2 \quad (49)$$

Thus restricted, (48) gives the velocity of z_0 :

$$\dot{z}_0 = \sqrt{2(E - V(z_0))} \quad (50)$$

Then we use this solution for the unperturbed system as a basis for a transformation where E is considered the new dependent variable, i.e. we let:

$$\dot{z} = \sqrt{2(E - V(z))}, \quad (51)$$

which gives:

$$E = \frac{1}{2} \dot{z}^2 + V(z) \Rightarrow \dot{E} = \left(\ddot{z} + \frac{dV}{dz} \right) \dot{z}, \quad (52)$$

or, substituting V from (47) and inserting into (43):

$$\begin{aligned} \dot{E} &= -\bar{h}_1 \dot{z}^2 - \bar{h}_2 \dot{z}^3 M(z) - \bar{h}_3 \dot{z}^4, \quad z \neq \frac{\pi}{2} + j\pi, \quad j = 0, 1, \dots \\ E_+ - E_- &= -(1 - R^2) \left(E_- - \frac{\pi^2}{8} \right), \quad z = \frac{\pi}{2} + j\pi. \end{aligned} \quad (53)$$

Dividing the first equation with \dot{z} and using (51), we obtain an equation where time is eliminated, and instead z takes the role of the independent variable:

$$\begin{aligned} \frac{dE}{dz} &= -\bar{h}_1 \sqrt{2(E - V(z))} - 2\bar{h}_2 (E - V(z)) M(z) - \bar{h}_3 (2(E - V(z)))^{3/2}, \quad z \neq \frac{\pi}{2} + j\pi \\ E_+ - E_- &= -(1 - R^2) \left(E_- - \frac{\pi^2}{8} \right), \quad z = \frac{\pi}{2} + j\pi, \end{aligned} \quad (54)$$

Under assumptions (46) the system has the general form (9), and can thus be averaged using (10), giving:

$$\begin{aligned} \frac{dE_1}{dz} &= q(E_1) \\ q(E_1) &= -\bar{h}_1 \left\{ \frac{1}{2} \sqrt{2E_1 - \frac{\pi^2}{4}} + \frac{2}{\pi} E_1 \arcsin \left(\frac{\pi}{2\sqrt{2E_1}} \right) \right\} - \frac{1 - R^2}{\pi} \left(E_1 - \frac{\pi^2}{8} \right) \\ &\quad - \bar{h}_3 \left\{ \left(2E_1 - \frac{\pi^2}{4} \right)^{3/2} + \frac{3}{4} E_1 \sqrt{2E_1 - \frac{\pi^2}{4}} + \frac{3}{\pi} E_1^2 \arcsin \left(\frac{\pi}{2\sqrt{2E_1}} \right) \right\}. \end{aligned} \quad (55)$$

Stationary solutions of this determines periodic oscillations of the mass on the belt with two impacts per oscillation period. The physical meaning can be illustrated by considering the case $h_3 = \bar{h}_3 = 0$ (which implies $h_2 = \bar{h}_2 = 0$), i.e. friction is monotonically decreasing with increased interface velocity. In that case increasing amplitudes of self-excited oscillations cannot be limited by increased friction, but solely by the hard stops. Then the mass gains energy during slipping and dissipates it during impacts. If the energy obtained during slipping exceeds what is lost during impact, the total energy will increase. But the oscillation amplitudes cannot exceed the fixed clearance width 2Δ , so increased system energy can only go into increased velocity, and correspondingly increased oscillation frequency. Thus, when friction-induced oscillations are first initiated, their amplitude will build up until the mass starts hitting the stops, whereafter the frequency of oscillations increase until a balance between gained and dissipated energy is attained.

To calculate the frequency of stationary oscillations we first determine the corresponding stationary energy \tilde{E}_1 as a solution of $q(\tilde{E}_1) = 0$. Then the corresponding oscillation period \tilde{T} (equal to twice the free-flight time between two successive impacts) and frequency $\tilde{\omega} = 2\pi/\tilde{T}$ is calculated from (51), which is valid in-between two impacts, $z \in]-\pi/2; \pi/2[$:

$$\frac{dz}{dt} = \sqrt{2(\tilde{E} - V(z))} \Rightarrow \tilde{T} = 2 \int_{z=-\frac{\pi}{2}}^{z=\frac{\pi}{2}} dt = 2 \int_{-\frac{\pi}{2}}^{\frac{\pi}{2}} \frac{dz}{\sqrt{2(\tilde{E} - V(z))}}, \quad (56)$$

which, by inserting (47) and (24) and integrating, gives:

$$\tilde{\omega} = \frac{2\pi}{\tilde{T}} = \left(\frac{2}{\pi} \arcsin \left(\frac{\pi}{2} / \sqrt{2\tilde{E}} \right) \right)^{-1} \quad (57)$$

Fig. 11 illustrates how the stationary oscillation frequency computed by this expression increases with the energy input parameter ($-h_1$) for parameters as given in the legend. As appears the approximate results (in solid line) agree asymptotically with numerical simulation (circles) of the original system (43) for small values of $|h_1|$, i.e. as the assumptions (46) are better fulfilled.

5. Second-order analysis

It is a common experience with nonlinear systems, demonstrated also by the examples in Section 4, that essential system behavior is revealed by approximate analysis to lowest (i.e. first) order. However, higher order analysis may be necessary when higher numerical accuracy is required, or if parameters that are assumed small are not really so, or if certain phenomena are only revealing themselves at higher order. The general averaging method for viro-impact analysis described in Section 3 can be systematically extended to any order of

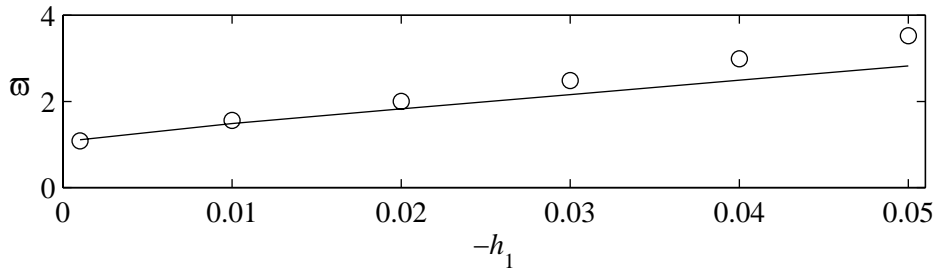


Fig. 11. Stationary oscillation frequency for a friction oscillator hitting two stops, as given by the analytical approximation (57) (solid line), and by numerical simulation of the original system (43) (circles). Parameters: $\Delta = 1$, $R = 0.95$, $h_2 = h_3 = 0$.

accuracy required, i.e. $\mathbf{x}=\mathbf{x}_1+\varepsilon\mathbf{x}_2+\dots$, though the computational burden increases rapidly with accuracy order. Of primary interest is here to improve the accuracy of the slowly changing variable \mathbf{x}_1 , while increased accuracy in the small and rapidly oscillating motions $\varepsilon\mathbf{x}_2$ is interesting only by its effect on \mathbf{x}_1 . In the first section below we derive second-order averaging results for a general vibro-impact system; in by-passing this also proves the first-order results stated in Section 3. Section 5.2 then provides, as an illustrative example, a second-order analysis of the self-excited friction oscillator with a one-sided stop, which was analyzed to first order in Section 4.3.

5.1. Generalized second-order averaging (for discontinuous systems)

This general second-order analysis was first published in [2], and is summarized here for completeness, proving first-order result as well. It holds for the following general system, which is an extension of (9) with second-order terms explicitly taken into account:

$$\begin{aligned} \frac{d\mathbf{x}}{d\varphi} &= \varepsilon\mathbf{f}_1(\mathbf{x},\varphi) + \varepsilon^2\mathbf{f}_2(\mathbf{x},\varphi) \text{ for } \varphi \neq j\pi, j=0,1,\dots, \mathbf{x}(\varphi) \in D \subset R^n, \varepsilon \ll 1 \\ \mathbf{x}_+ - \mathbf{x}_- &= \varepsilon\mathbf{g}_1(\mathbf{x}_-) + \varepsilon^2\mathbf{g}_2(\mathbf{x}_-) \text{ for } \varphi = j\pi, \end{aligned} \quad (58)$$

where $\mathbf{f}_{1,2}$ are 2π -periodic in φ , $\mathbf{f}_{1,2}$ and $\mathbf{g}_{1,2}$ are bounded and Lipschitz-continuous in \mathbf{x} on $\mathbf{x} \in D \subset R^n$, and \mathbf{x}_- and \mathbf{x}_+ are the states \mathbf{x} immediately before and after the j 'th impact, corresponding to the independent variable taking on the values $\varphi = j\pi$.

As with the standard averaging theorem [11], the first step in deriving approximate solution to (58) which are asymptotically valid to order ε^2 as $\varepsilon \rightarrow 0$, is to perform a near-identity transformation of the dependent variable, i.e.:

$$\mathbf{x} = \mathbf{x}_1 + \varepsilon\mathbf{x}_2(\mathbf{x}_1, \varphi) + \varepsilon^2\mathbf{x}_3(\mathbf{x}_1, \varphi) + \dots \quad (59)$$

The purpose of this is to obtain an autonomous equation for the slowly changing variable \mathbf{x}_1 :

$$\frac{d\mathbf{x}_1}{d\varphi} = \varepsilon\mathbf{E}_1(\mathbf{x}_1) + \varepsilon^2\mathbf{E}_2(\mathbf{x}_1) + \dots, \quad (60)$$

where $\mathbf{x}_1(\varphi)$ remains continuous during impacts, i.e. $\mathbf{x}_{1+} = \mathbf{x}_{1-}$. Inserting (59) and (60) into (58) gives, when Taylor-expanding for small ε :

$$\varepsilon\mathbf{E}_1 + \varepsilon \frac{\partial \mathbf{x}_2}{\partial \varphi} + \varepsilon^2\mathbf{E}_2 + \varepsilon^2 \frac{\partial \mathbf{x}_2}{\partial \mathbf{x}_1} \mathbf{E}_1 + \varepsilon^2 \frac{\partial \mathbf{x}_3}{\partial \varphi} + \dots \quad (61)$$

$$= \varepsilon\mathbf{f}_1(\mathbf{x}_1, \varphi) + \varepsilon^2\mathbf{f}_2(\mathbf{x}_1, \varphi) + \varepsilon^2 \frac{\partial \mathbf{f}_1(\mathbf{x}_1, \varphi)}{\partial \mathbf{x}_1} \mathbf{x}_2 + \dots, \quad \varphi \neq j\pi$$

$$\begin{aligned} \varepsilon\mathbf{x}_{2+} + \varepsilon^2\mathbf{x}_{3+} + \dots - \varepsilon\mathbf{x}_{2-} - \varepsilon^2\mathbf{x}_{3-} - \dots \\ = \varepsilon\mathbf{g}_1(\mathbf{x}_1) + \varepsilon^2 \frac{\partial \mathbf{g}_1(\mathbf{x}_1)}{\partial \mathbf{x}_1} \mathbf{x}_{2-} + \varepsilon^2\mathbf{g}_2(\mathbf{x}_1) \dots, \quad \varphi = j\pi. \end{aligned} \quad (62)$$

Balancing terms with similar powers of ε then gives the following equations for the unknown functions \mathbf{x}_2 and \mathbf{x}_3 , respectively:

$$\begin{aligned} \frac{\partial \mathbf{x}_2}{\partial \varphi} &= \mathbf{f}_1(\mathbf{x}_1, \varphi) - \mathbf{E}_1, \quad \varphi \neq j\pi \\ \mathbf{x}_{2+} - \mathbf{x}_{2-} &= \mathbf{g}_1(\mathbf{x}_1), \quad \varphi = j\pi, \end{aligned} \quad (63)$$

and

$$\begin{aligned}\frac{\partial \mathbf{x}_3}{\partial \varphi} &= \mathbf{f}_2(\mathbf{x}_1, \varphi) + \frac{\partial \mathbf{f}_1(\mathbf{x}_1, \varphi)}{\partial \mathbf{x}_1} \mathbf{x}_2 - \mathbf{E}_2 - \frac{\partial \mathbf{x}_2}{\partial \mathbf{x}_1} \mathbf{E}_1, \quad \varphi \neq j\pi \\ \mathbf{x}_{3+} - \mathbf{x}_{3-} &= \frac{\partial \mathbf{g}_1(\mathbf{x}_1)}{\partial \mathbf{x}_1} \mathbf{x}_{2-} + \mathbf{g}_2(\mathbf{x}_1), \quad \varphi = j\pi.\end{aligned}\tag{64}$$

This could be continued to the equation for \mathbf{x}_n corresponding to any order ε^{n-1} of accuracy, so that for n th-order analysis one includes equations up to \mathbf{x}_{n+1} .

The above balancing of terms only makes sense if the functions \mathbf{x}_1 and \mathbf{x}_2 remain bounded in time; otherwise terms of the same order of ε would run into different magnitude orders after some time. We are at the liberty to impose restrictions on variables that will prevent this, since (59)-(60) introduces more new variables than present in the original system (58). Thus, to ensure \mathbf{x}_1 and \mathbf{x}_2 are bounded, we may require the average rate of change of these functions with φ to vanish. For the function \mathbf{x}_2 the average becomes, using (63) and (7):

$$\begin{aligned}\left\langle \frac{\partial \mathbf{x}_2}{\partial \varphi} \right\rangle_{\varphi} &= \frac{1}{2\pi} \left[\int_{0^+}^{\pi} (\mathbf{f}_1(\mathbf{x}_1, \varphi) - \mathbf{E}_1) d\varphi + \mathbf{g}_1(\mathbf{x}_1) + \int_{\pi^+}^{2\pi} (\mathbf{f}_1(\mathbf{x}_1, \varphi) - \mathbf{E}_1) d\varphi + \mathbf{g}_1(\mathbf{x}_1) \right] \\ &= \langle \mathbf{f}_1(\mathbf{x}_1, \varphi) \rangle - \mathbf{E}_1 + \frac{\mathbf{g}_1(\mathbf{x}_1)}{\pi},\end{aligned}\tag{65}$$

Here the terms $\mathbf{g}_1(\mathbf{x}_1)$ result from integrating $\partial \mathbf{x}_2 / \partial \varphi$ over the impact times, using the second equation in (63), e.g., at $\varphi = \pi$. $\int_{\pi^-}^{\pi^+} (\partial \mathbf{x}_2 / \partial \varphi) d\varphi = \int_{\mathbf{x}_2(\pi^-)}^{\mathbf{x}_2(\pi^+)} d\mathbf{x}_2 = \mathbf{x}_{2+} - \mathbf{x}_{2-} = \mathbf{g}_1(\mathbf{x}_1)$, where it should be recalled that the slow function $\mathbf{x}_1(\varphi)$ remains continuous during impacts (cf. remark under (60)). Thus, according to (65) the rate of change of \mathbf{x}_2 vanishes when:

$$\mathbf{E}_1 = \langle \mathbf{f}_1(\mathbf{x}_1, \varphi) \rangle_{\varphi} + \pi^{-1} \mathbf{g}_1(\mathbf{x}_1).\tag{66}$$

Similarly, by (64) the condition for $\langle \partial \mathbf{x}_3 / \partial \varphi \rangle_{\varphi}$ to vanish becomes:

$$\mathbf{E}_2 = \left\langle \mathbf{f}_2(\mathbf{x}_1, \varphi) + \frac{\partial \mathbf{f}_1(\mathbf{x}_1, \varphi)}{\partial \mathbf{x}_1} \mathbf{x}_2 - \frac{\partial \mathbf{x}_2}{\partial \mathbf{x}_1} \mathbf{E}_1 \right\rangle_{\varphi} + \frac{1}{2\pi} \frac{\partial \mathbf{g}_1(\mathbf{x}_1)}{\partial \mathbf{x}_1} (\mathbf{x}_{2-}(0) + \mathbf{x}_{2-}(\pi)) + \frac{\mathbf{g}_2(\mathbf{x}_1)}{\pi}.\tag{67}$$

To calculate \mathbf{E}_2 we first need to determine \mathbf{x}_2 by integrating (63); this gives:

$$\begin{aligned}\mathbf{x}_2 &= \int_0^{\varphi} (\mathbf{f}_1(\mathbf{x}_1, \eta) - \mathbf{E}_1(\mathbf{x}_1)) d\eta + \mathbf{c}(\mathbf{x}_1), \quad \varphi \neq j\pi \\ \mathbf{x}_{2+} &= \mathbf{x}_{2-} + \mathbf{g}_1(\mathbf{x}_1), \quad \varphi = j\pi,\end{aligned}\tag{68}$$

where the function $\mathbf{c}(\mathbf{x}_1)$ can be chosen arbitrarily, e.g. by requiring the average of \mathbf{x}_2 between the discontinuities to vanish, giving:

$$\mathbf{c}(\mathbf{x}_1) = - \left\langle \int_0^{\varphi} (\mathbf{f}_1(\mathbf{x}_1, \eta) - \mathbf{E}_1(\mathbf{x}_1)) d\eta \right\rangle_{\varphi}.\tag{69}$$

With this inserted into (68) one finds that the term $\langle (\partial \mathbf{x}_2 / \partial \mathbf{x}_1) \mathbf{E}_1 \rangle$ in (67) vanishes, so that:

$$\mathbf{E}_2 = \left\langle \mathbf{f}_2(\mathbf{x}_1, \varphi) + \frac{\partial \mathbf{f}_1(\mathbf{x}_1, \varphi)}{\partial \mathbf{x}_1} \mathbf{x}_2 \right\rangle_{\varphi} + \frac{1}{2\pi} \frac{\partial \mathbf{g}_1(\mathbf{x}_1)}{\partial \mathbf{x}_1} (\mathbf{x}_{2-}(0) + \mathbf{x}_{2-}(\pi)) + \pi^{-1} \mathbf{g}_2(\mathbf{x}_1).\tag{70}$$

In summary, to second order the solutions of (58) are given by the first two terms of (59),

where \mathbf{x}_1 is the solution of the autonomous system (60), \mathbf{x}_2 is given by (68)-(69), \mathbf{E}_1 by (66), and \mathbf{E}_2 by (70). The accuracy of this approximation can be estimated as for standard averaging (cf. [2], Appendix V): The error $\|(\mathbf{x}_1 + \varepsilon \mathbf{x}_2) - \mathbf{x}\|$ is $O(\varepsilon^2)$ on the time-scale $1/\varepsilon$ (on which scale the error of *first* order analysis is $O(\varepsilon)$, cf. Section 3.3).

A remark on the meaning of ‘‘approximation order’’ may be necessary: The first-order approximation to \mathbf{x} is given by the first term \mathbf{x}_1 of (59), while the second-order approximation to \mathbf{x} includes also \mathbf{x}_2 . But as appears from (60), \mathbf{x}_1 *per se* can be calculated at varying levels accuracy, i.e. $\mathbf{x}_1 = \mathbf{x}_{11} + \varepsilon \mathbf{x}_{12} + O(\varepsilon^2)$. If increased accuracy is in need, it is typically a better approximation for the slowly changing variable \mathbf{x}_1 that is needed, while the increased accuracy in the small and rapidly oscillating motions \mathbf{x}_2 is interesting only by its effect on \mathbf{x}_1 . Thus, ‘‘the second-order approximation to \mathbf{x}_1 ’’ implies the determination of \mathbf{x}_1 with terms to order ε^2 included.

Note that the first-order approximation to \mathbf{x}_1 (equal to \mathbf{x}_{11} mentioned above) is determined from (60) truncated at the first (ε^1) term, and with \mathbf{E}_1 given by (66). This system is identical to (10), and thus the first-order averaging procedure for discontinuous systems used in Section 3.3 is also proved.

5.2. Example: 2nd-order analysis of a self-excited friction oscillator with a one-sided stop

As an example we reconsider the friction oscillator with a one-sided stop of Section 4.3. To illustrate using second-order analysis to calculate stationary oscillation amplitudes, we start from the van der Pol transformed modulation equations (37) of the system, insert $\dot{\theta} = \dot{\psi} - 1$ from (15), and divide the A -equation with the resulting ψ -equation to obtain a system where ψ takes the role of the independent variable:

$$\frac{dA}{d\psi} = \frac{(\Delta + h_2 A^2 \cos^2 \psi) \cos \psi \operatorname{sgn}(\sin \psi) - (h_1 + h_3 A^2 \cos^2 \psi) A \cos^2 \psi}{1 - \left(\frac{\Delta}{A} + h_2 A \cos^2 \psi \right) |\sin \psi| + (h_1 + h_3 A^2 \cos^2 \psi) \cos \psi \sin \psi}, \quad \psi \neq j\pi \quad (71)$$

$$A_+ - A_- = -(1 - R)A_-, \quad \psi = j\pi.$$

With small parameters as assumed in (34), the expression for $dA/d\psi$ has the form $\varepsilon f_1/(1 + \varepsilon f_2)$, whose second-order Taylor-expansion for small ε is $\varepsilon f_1 - (\varepsilon f_1)(\varepsilon f_2)$. Thus (71) can be written in the general form (58) with $n = 1$, $\mathbf{x} = A$, $\varphi = \psi$, and:

$$\begin{aligned} \varepsilon \mathbf{f}_1(\mathbf{x}, \varphi) &= \varepsilon f_1(A, \psi) \\ &= (\Delta + h_2 A^2 \cos^2 \psi) \cos \psi \operatorname{sgn}(\sin \psi) - (h_1 + h_3 A^2 \cos^2 \psi) A \cos^2 \psi \\ \varepsilon \mathbf{f}_2(\mathbf{x}, \varphi) &= \varepsilon^2 f_2(A, \psi) \end{aligned} \quad (72)$$

$$\begin{aligned} &= \varepsilon f_1(A, \psi) \left[\left(\frac{\Delta}{A} + h_2 A \cos^2 \psi \right) |\sin \psi| - (h_1 + h_3 A^2 \cos^2 \psi) \cos \psi \sin \psi \right] \\ \varepsilon \mathbf{g}_1(\mathbf{x}_-) &= \varepsilon g_1(A_-) = -(1 - R)A_- \\ \varepsilon^2 \mathbf{g}_2(\mathbf{x}_-) &= 0. \end{aligned} \quad (73)$$

Next, to calculate an approximate solution of the form (59)-(60), i.e.:

$$A = A_1 + \varepsilon A_2(A_1, \psi) + \varepsilon^2 A_3(A_1, \psi) + \dots \quad (74)$$

$$\frac{dA_1}{d\psi} = \varepsilon E_1(A_1) + \varepsilon^2 E_2(A_1) + \dots, \quad (75)$$

we use (66), (68)-(69), and (70) to compute:

$$\mathbf{E}_1(\mathbf{x}_1) = E_1(A_1) = \langle f_1(A_1, \psi) \rangle_\psi + \pi^{-1} g_1(A_1) = -\left(\frac{1}{2}h_1 + \frac{1-R}{\pi}\right)A_1 - \frac{3}{8}h_3A_1^3 \quad (76)$$

$$\mathbf{c}(\mathbf{x}_1) = c(A_1) = -\left\langle \int_0^\psi (f_1(A_1, \eta) - E_1(A_1)) d\eta \right\rangle_\psi = -\frac{2}{\pi}\Delta - \frac{14}{9\pi}h_2A_1^2 - (1-R)A_1 \quad (77)$$

$$\begin{aligned} \mathbf{x}_2 = A_2 &= \int_0^\psi (f_1(A_1, \eta) - E_1(A_1)) d\eta + c(A_1) \\ &= \left(\Delta + \frac{5}{6}h_2A_1^2 \left(1 + \frac{1}{5}\cos 2\psi\right)\right) |\sin \psi| - \frac{1}{4}\left(h_1A_1 + \left(1 + \frac{1}{4}\cos 2\psi\right)h_3A_1^3\right) \sin 2\psi \\ &\quad + \frac{1-R}{\pi}A_1\psi + c(A_1), \quad \psi \neq j\pi \end{aligned} \quad (78)$$

$$\begin{aligned} \mathbf{x}_{2+} = A_{2+} &= A_{2-} - (1-R)A_1, \quad \psi = j\pi \\ \mathbf{E}_2 = E_2 &= \left\langle f_2(A_1, \psi) + \frac{\partial f_1(A_1, \psi)}{\partial A_1} A_2 \right\rangle_\psi + \frac{1}{2\pi} \frac{\partial g_1(A_1)}{\partial A_1} (A_{2-}(0) + A_{2-}(\pi)) + \pi^{-1} g_2(A_1) \\ &= \frac{\Delta}{\pi} \left(-h_1 + \frac{1}{4}h_3A_1^2 + \frac{2}{\pi}(1-R)\right) - \frac{1}{\pi}h_1h_2A_1^2 - \frac{7}{20\pi}h_2h_3A_1^4 + \frac{1-R}{\pi}A_1 \left(\frac{1-R}{2} - \frac{14}{9\pi}h_2A_1\right). \end{aligned} \quad (79)$$

Stationary oscillation amplitudes $A_1(t) = A_{1\infty}$ are determined as the stationary solutions to (75), i.e. we let $dA_1/d\psi = 0$ and solve for A_1 :

$$\varepsilon E_1(A_{1\infty}) + \varepsilon^2 E_2(A_{1\infty}) + \dots = 0, \quad (80)$$

To find non-trivial solutions $A_{1\infty} \neq 0$, corresponding to self-excited oscillations of the mass, we let:

$$A_{1\infty} = A_{11\infty} + \varepsilon A_{12\infty} + \dots, \quad (81)$$

and Taylor-expand (80) for small ε :

$$E_1(A_{11\infty}) + \varepsilon \left(\frac{dE_1}{dA_{1\infty}} \Big|_{A_{1\infty}=A_{11\infty}} A_{12\infty} + E_2(A_{11\infty}) \right) = O(\varepsilon^2). \quad (82)$$

Balancing terms with similar powers of ε then gives:

$$E_1(A_{11\infty}) = 0 \quad (83)$$

$$A_{12\infty} = \frac{-E_2(A_{11\infty})}{dE_1/dA_1|_{A_1=A_{11\infty}}}, \quad (84)$$

which on inserting (76) for E_1 gives the non-trivial solution:

$$A_{11\infty} = \sqrt{-\frac{8\hat{\beta}}{3h_3}}, \quad \hat{\beta} = \frac{h_1}{2} + \frac{1-R}{\pi}, \quad (85)$$

which is identical to the first-order approximation (40) already calculated in Section 4.3. The expression for $A_{12\infty}$ in (84) is evaluated by inserting (79) for E_2 , and calculating the derivative of E_1 by using (76):

$$\frac{dE_1}{dA_1} = -\left(\frac{1}{2}h_1 + \frac{1-R}{\pi} + \frac{9}{8}h_3A_1^2\right). \quad (86)$$

Inserting particular values for R , Δ , h_1 , h_2 , and h_3 , one then calculates the second-order approximate oscillation amplitudes $A_{1\infty}$ from (81), by first calculating the first-order approximation $A_{11\infty}$ from (85), and to that add the second-order correction $A_{12\infty}$ given by (84) with (86) and (79) inserted.

Fig. 9 and Fig. 10 illustrate how the second-order approximate results (dotted line) agree better with numerical simulation (dashed line / circles) than does the first-order approximation (solid line). The quantitative agreement between second-order results and simulation is seen to be good, though lesser so for the higher values of $|\Delta|$, as could be expected from the asymptotic nature of the predictions and the assumptions (34).

Fig. 12 shows the errors in stationary oscillation amplitudes as a function of Δ for the first- and second-order approximations (circles and squares, respectively); As appears the errors are of the theoretically estimated magnitude orders: Δ (solid line) and Δ^2 (dashed), respectively).

This section demonstrates that second-order discontinuous averaging analysis is applicable and more accurate, but also much more elaborate.

6. Summary and conclusions

An extended form of first-order averaging can be used for analyzing vibro-impact problems with near-elastic impact. This can be accomplished by a discontinuous transformation of variables that converts large velocity-discontinuities into small ones, followed by yet a transformation to a system of a given standard form (9), which can be averaged. The first-order averaged system, as given by (10), is a set of ordinary differential equations valid at all times. Typically it is much simpler than the original system, so that established standard procedures can be used for deriving analytical expressions for key properties such as stationary oscillation amplitudes and frequencies, or slow components of motion. This was demonstrated above for unforced harmonic oscillators, and for self-excited friction oscillators with one- or two-sided hard stops. Also, in [2,3] the same technique is used to analyze nonlinear responses for resonantly excited harmonic oscillators with one- or two-sided stops. In particular when nonlinearities additional to those caused by impact are involved, this procedure seems simpler than alternatives such as mapping- or stitching-analysis.

Based on the extended averaging theorem for discontinuous systems [2,3], the procedure has stronger mathematical support than the methods of harmonic linearization [1] and direct separation of motions [10]. The accuracy of obtained approximate solutions can be estimated *a priori*, and improved to any order required by a systematic procedure. The paper presents first- as well as second-order general procedures and results, and demonstrates by several

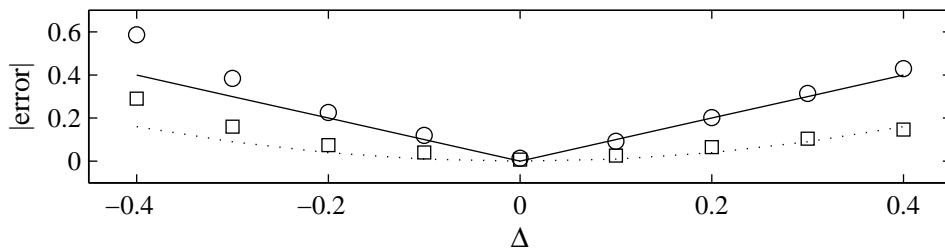


Fig. 12. Absolute error in stationary amplitudes as a function of the distance Δ from the (unstable) equilibrium of the mass on a moving belt to the hard stop: Errors of the first-order approximation (40) (circles) compared to $|\Delta|$ (solid line), and errors of the second-order approximation (81) (squares) compared to Δ^2 (dotted line). Parameters as for Fig. 9.

examples that errors are of the estimated small magnitude order, when the assumptions for this are fulfilled. First-order analysis is reasonably simple and may be accurate enough for many purposes, as illustrated in the examples. Higher-order analysis is considerably more elaborate, though strictly systematic, and to some extent automatizable using symbolic computation software.

The key step and problem in using discontinuous averaging for vibro-impact problems is to find a suitable, discontinuity-reducing transformation for the application at hand. The example systems and transformations used for illustration in this paper and in [2,3] are varied, and may cover a broad range of applications, as well as providing starting points for quite other types of systems. However, it would be useful to more systematically identify different classes of vibro-impact systems, and finding corresponding workable transformations. Also, with the present paper focusing on describing the procedure and illustrate its use, it seems relevant in the future to compare it with alternatives, considering aspects such as range of applicability, accuracy, reliability, and ease of use.

References

- [1] V.I. Babitsky, *Theory of Vibro-Impact Systems and Applications*, Springer-Verlag, Berlin, 1998.
- [2] A. Fidlin, *Nonlinear Oscillations in Mechanical Engineering*, Springer-Verlag, Berlin Heidelberg, 2005.
- [3] A. Fidlin, On the strongly nonlinear behavior of an oscillator in a clearance, in: D.H. van Campen, M.D. Lazurko, W.P.J.M. van der Oever (Eds.), *Proceedings of ENOC-2005*, Eindhoven, Netherlands, 7-12 August 2005, Technical University of Eindhoven, 2005, pp. 389-398.
- [4] J.J. Thomsen, Slow high-frequency effects in mechanics: problems, solutions, potentials, *International Journal of Bifurcation and Chaos* 15 (2005) 2799-2818.
- [5] J.J. Thomsen, A. Fidlin, Discontinuous transformations and averaging for vibro-impact analysis, in: W. Gutkowski, T.A. Kowalewski (Eds.), *ICTAM04 Abstracts Book and CD-ROM Proceedings*, XXI Int. Congress of Theoretical and Applied Mechanics, IPPT PAN, Warsaw, 2004, p. 2 pp. (CDROM ID: SM25L_12694).
- [6] A.E. Kobrinskii, *Dynamics of Mechanisms with Elastic Connections and Impact Systems*, Iliffe Books, London, 1969.
- [7] A. Fidlin, *On the Oscillations in Discontinuous and Unconventionally Strong Excited Systems: Asymptotic Approaches and Dynamic Effects*, doctoral dissertation, University of Karlsruhe, Dept. of Mechanical Engineering, 2002.
- [8] V.F. Zhuravlev, D.M. Klimov, *Applied Methods in the Theory of Nonlinear Oscillations (in Russian)*, Nauka, Moscow, 1988.
- [9] A.P. Ivanov, *Dynamics of Systems with Mechanical Collisions (in Russian)*, International Program of Education, Moscow, 1997.
- [10] I.I. Blekhman, *Vibrational Mechanics - Nonlinear Dynamic Effects, General Approach, Applications*, World Scientific, Singapore, 2000.
- [11] J.A. Sanders, F. Verhulst, *Averaging Methods in Nonlinear Dynamical Systems*, Springer-Verlag, New York, 1985.
- [12] N.N. Bogoliubov, Y.A. Mitropolskii, *Asymptotic Methods in the Theory of Nonlinear Oscillations*, Gordon and Breach, New York, 1961.
- [13] A.H. Nayfeh, *Perturbation Methods*, Wiley, New York, 1973.
- [14] J.J. Thomsen, *Vibrations and Stability: Advanced Theory, Analysis, and Tools*, Springer-Verlag, Berlin Heidelberg, 2003.
- [15] V.F. Zhuravlev, Method of analysis of vibration-shock systems by means of special functions (in Russian), *Izv Akad Nauk (SSSR) Mekh Tverd Tela* No. 2 (1976) 30-34.
- [16] V.F. Zhuravlev, An investigation of some vibroimpact systems by the method of non-smooth transformations (in Russian), *Izv Akad Nauk (SSSR) Mekh Tverd Tela* No. 6 (1977) 24-28.

- [17] V.F. Zhuravlev, A.I. Meniailov, An investigation of a vibroimpact system with limited excitation (in Russian), *Izv Akad Nauk (SSSR) Mekh Tverd Tela* No. 2 (1978) 45-50.
- [18] A.Y. Fidlin, On averaging in systems with a variable number of degrees of freedom, *Journal of Applied Mathematics and Mechanics* 55 (1991) 507-510.
- [19] A.V. Pechenev, A.Y. Fidlin, Hierachy of resonant motions excited in a vibroimpact system with contact zones by an inertial source of limited power, *Izv. AN SSSR. Mekhanika Tverdogo Tela (English Translation)* 27 (1992) 46-53.
- [20] V.N. Pilipchuk, Some remarks on non-smooth transformations of space and time for vibrating systems with rigid barriers, *PMM Journal of Applied Mathematics and Mechanics* 66 (2002) 31-37.
- [21] A. Fidlin, On the averaging of discontinuous systems, in: I.I. Blekhman (Ed.), *Selected Topics in Vibrational Mechanics*, World Scientific, Singapore, 2003, pp. 357-402.
- [22] M.F. Dimentberg, D.V. Iourtchenko, Random vibrations with impacts: a review, *Nonlinear Dynamics* 36 (2004) 229-254.
- [23] Y.G. Panovko, I.I. Gubanova, *Stability and Oscillations of Elastic Systems; Paradoxes, Fallacies and New Concepts*, Consultants Bureau, New York, 1965.
- [24] J.J. Thomsen, A. Fidlin, Analytical approximations for stick-slip vibration amplitudes, *International Journal of Non-linear Mechanics* 38 (2003) 389-403.
- [25] R.A. Ibrahim, Friction-induced vibration, chatter, squeal, and chaos: part II - dynamics and modeling, *Friction-induced vibration, chatter, squeal, and chaos, ASME DE-Vol 49* (1992) 123-138.

The DCAMM reports are issued for early dissemination of research results from the Department of Mechanical Engineering, Department of Mathematics, and Department of Informatics and Mathematical Modelling at the Technical University of Denmark together with Institute of Mechanical Engineering and Building Technology and Structural Engineering at the Aalborg University. These technical reports are as a rule submitted to international scientific journals and should not be widely distributed until after the date of publication. Whenever possible reference should be given to the final publications and not to the DCAMM reports.

DANISH CENTER FOR APPLIED MATHEMATICS AND MECHANICS

Scientific Council

Martin P. Bendsøe	Dept. of Mathematics, DTU
Morten Brøns	Dept. of Mathematics, DTU
Esben Byskov	Building Technology and Structural Engineering, AAU
Jørgen Juncher Jensen	Dept. of Mechanical Eng., Maritime Engineering, DTU
Frithiof Niordson	Dept. of Mechanical Eng., Solid Mechanics, DTU
Niels Olhoff	Institute of Mechanical Engineering, AAU
Ole Sigmund	Dept. of Mechanical Eng., Solid Mechanics, DTU
Pauli Pedersen	Dept. of Mechanical Eng., Solid Mechanics, DTU
B. Mutlu Sumer	Dept. of Mechanical Eng., Coastal and River Eng., DTU
Jens Nørkær Sørensen	Dept. of Mechanical Eng., Fluid Mechanics, DTU
Per Grove Thomsen	Informatics and Mathematical Modelling, DTU
Ole Thybo Thomsen	Institute of Mechanical Engineering, AAU

Secretary

Ole Sigmund, Professor, dr. techn.
Department of Mechanical Engineering, Solid Mechanics
Nils Koppels Allé, Building 404
Technical University of Denmark
DK-2800 Kgs. Lyngby, Denmark